



中国科学院国家天文台
NATIONAL ASTRONOMICAL OBSERVATORIES, CAS

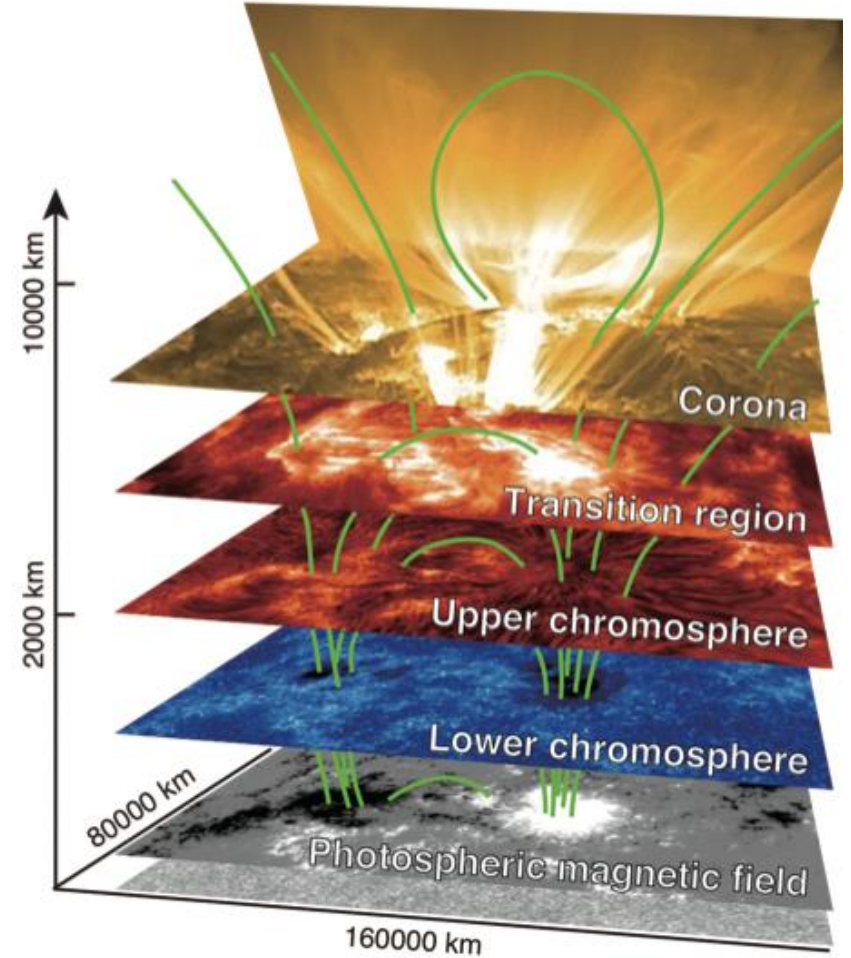
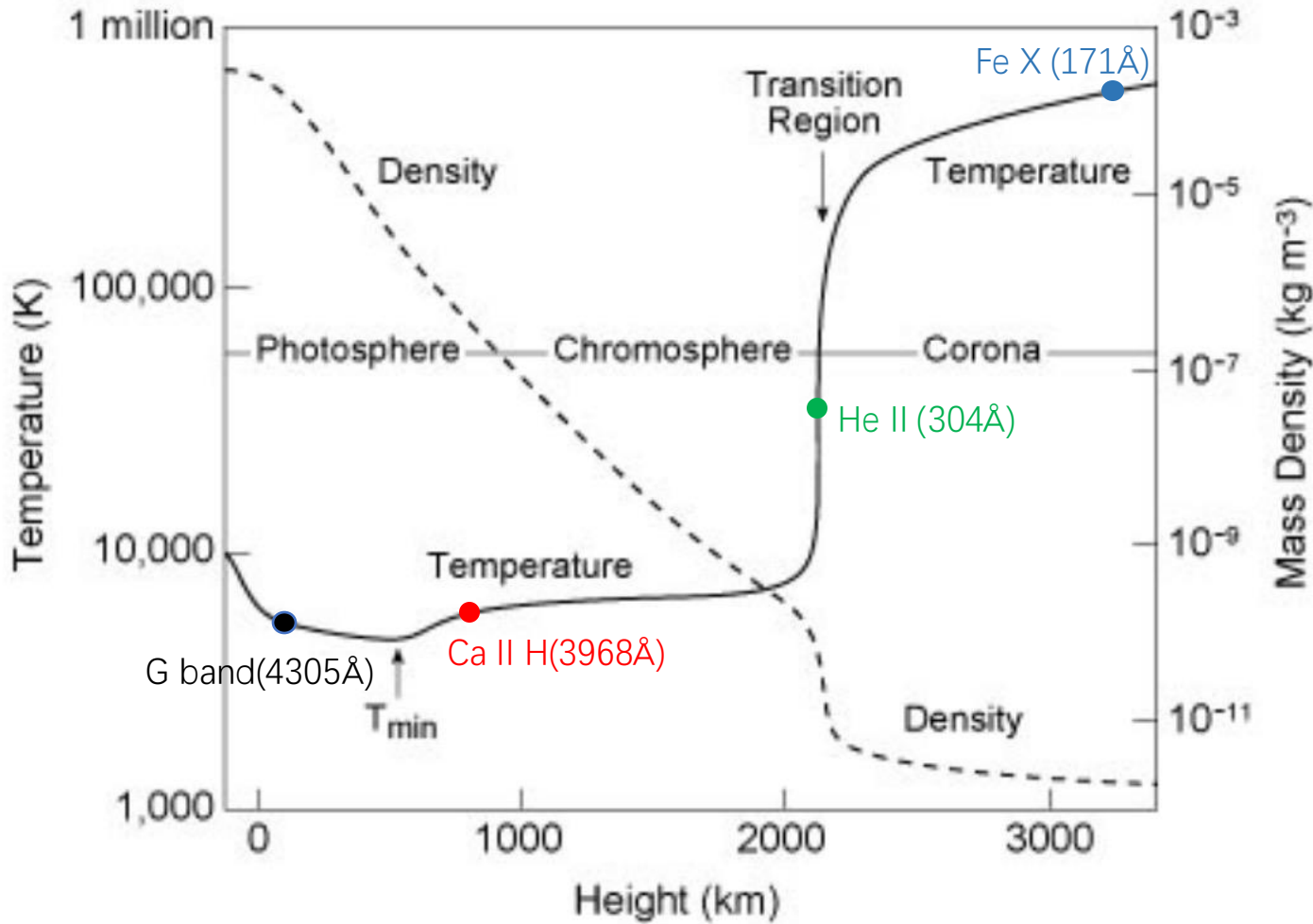
Atomic data for Solar Physics Applications

Wenxian Li

**National Astronomical Observatories
Chinese Academy of Sciences**

CompAS meeting, 2025.6.13, Lund, Sweden

Solar Atmosphere

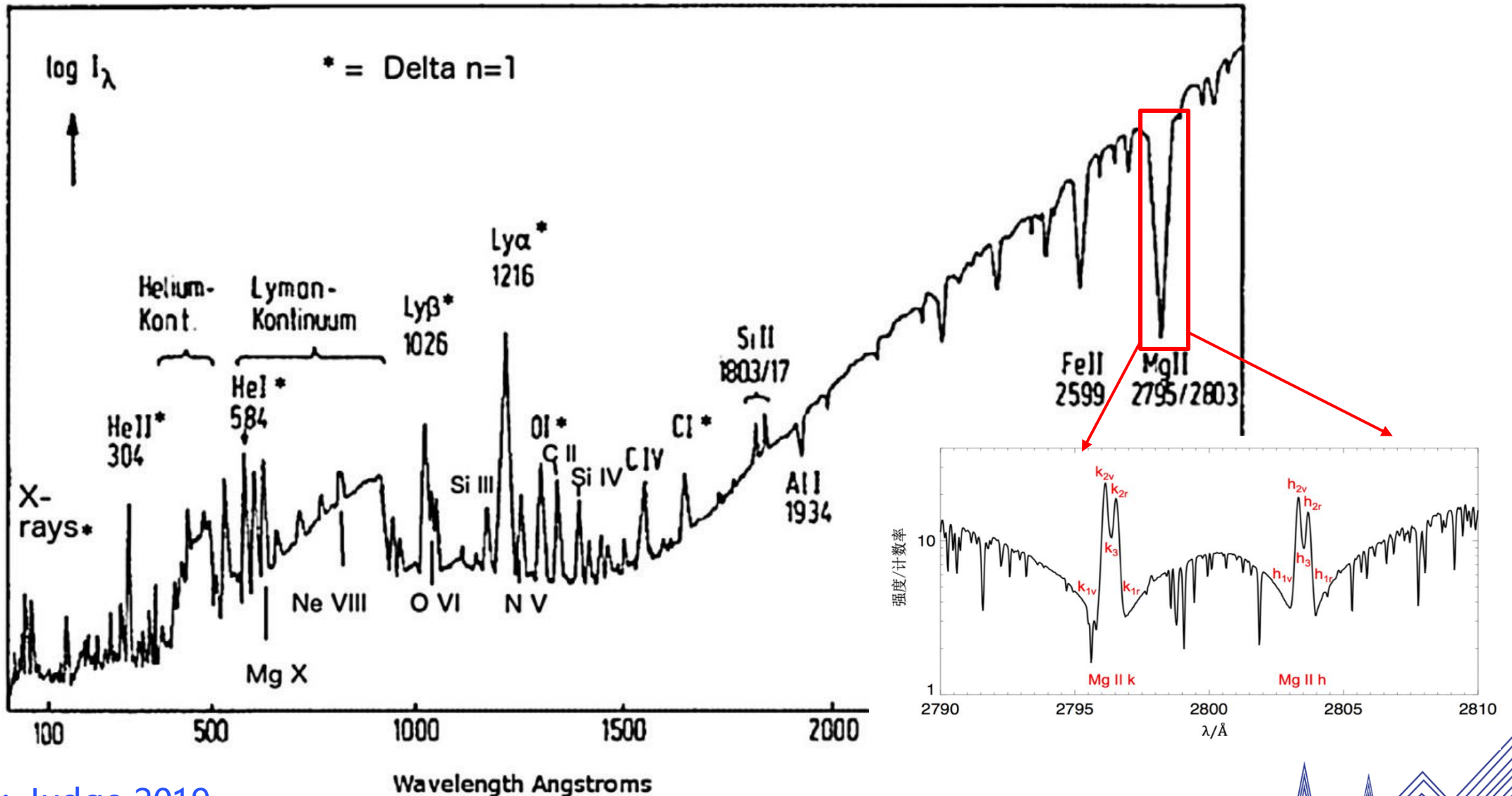


Source: Rajhans 2022

Credit: NAOJ/JAXA, NASA



Solar Spectra



Source: Judge 2019

Wavelength Angstroms

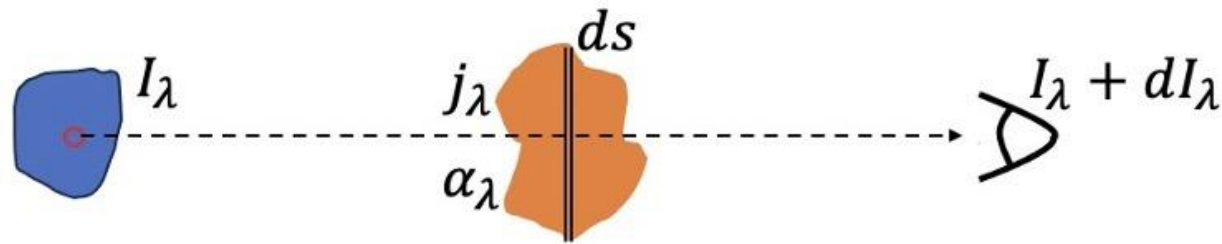


Solar Spectra Lines

Optical thin lines:
$$I(\lambda_{ji}) = \frac{h\nu_{ji}}{4\pi} \int N_j(Z^{+r}) A_{ji} ds \quad (\text{erg cm}^{-2} \text{ s}^{-1} \text{ sr}^{-1})$$

$$N_j(Z^{+r}) \equiv \frac{N_j(Z^{+r})}{N(Z^{+r})} \frac{N(Z^{+r})}{N(Z)} \frac{N(Z)}{N_H} \frac{N_H}{N_e} N_e$$

Optical thick lines:



emission

absorption

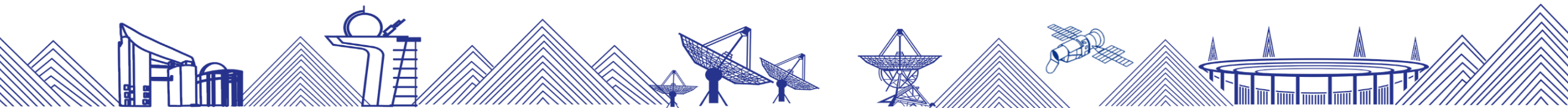
$$dI_\lambda(s) = j_\lambda(s) \rho ds - \kappa_\lambda(s) \rho I_\lambda(s) ds$$

statistical
equilibrium
+
radiative
transfer



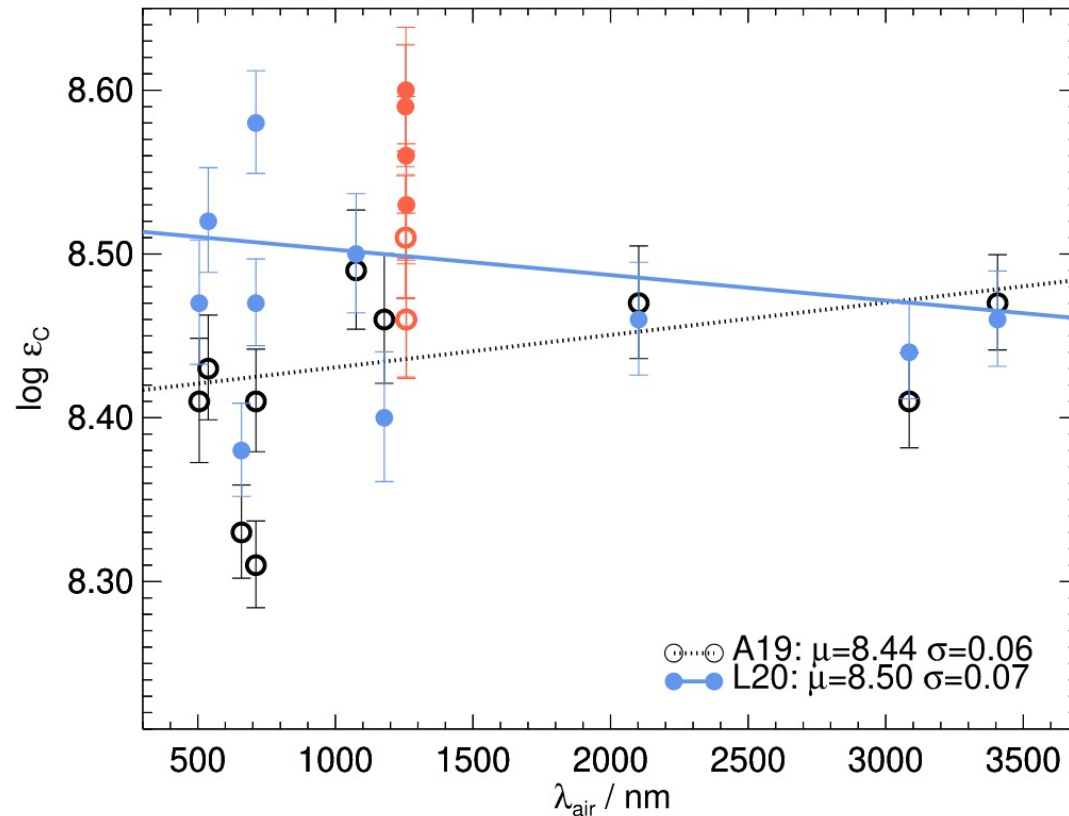
Atomic data

- wavelength
- radiative data $A/\log gf$
- collisional cross section
- photoionization cross section
- hyperfine and isotopic splitting
-

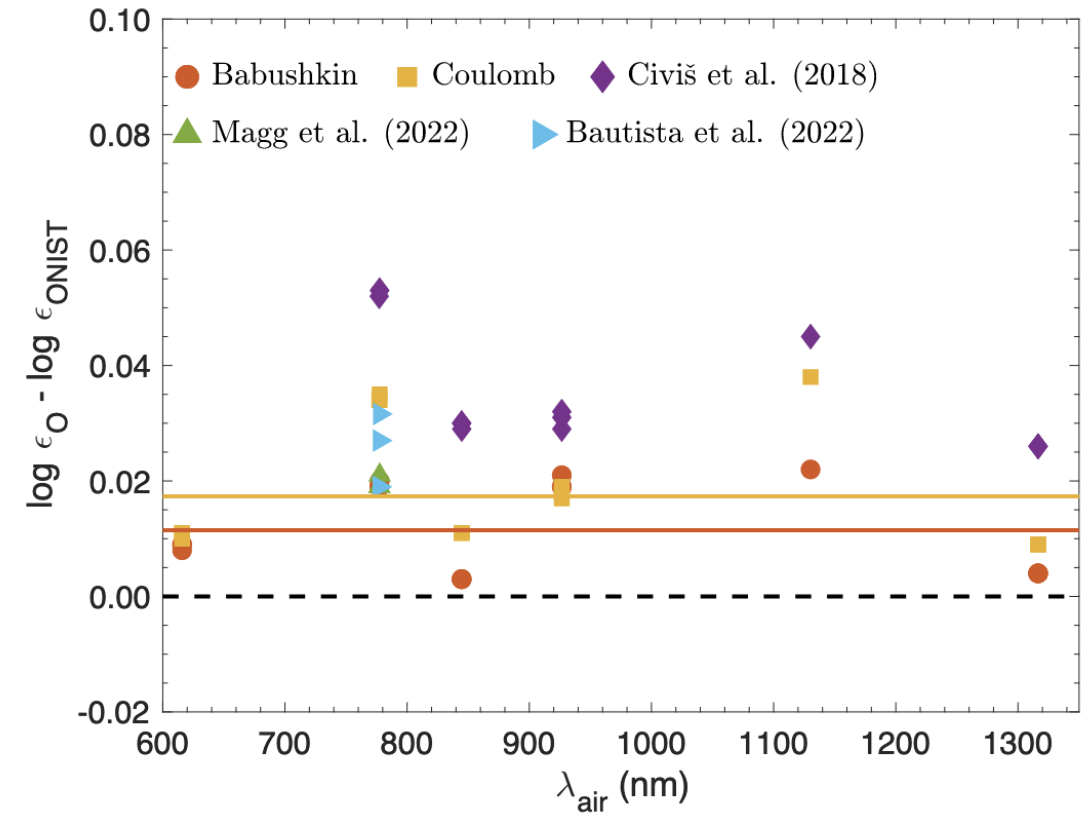


GRASP calculations for radiative transitions

Collaborated with Anish Amarsi, Per Jönsson, Meichun Li on C, N, O, S atoms and atomic ions



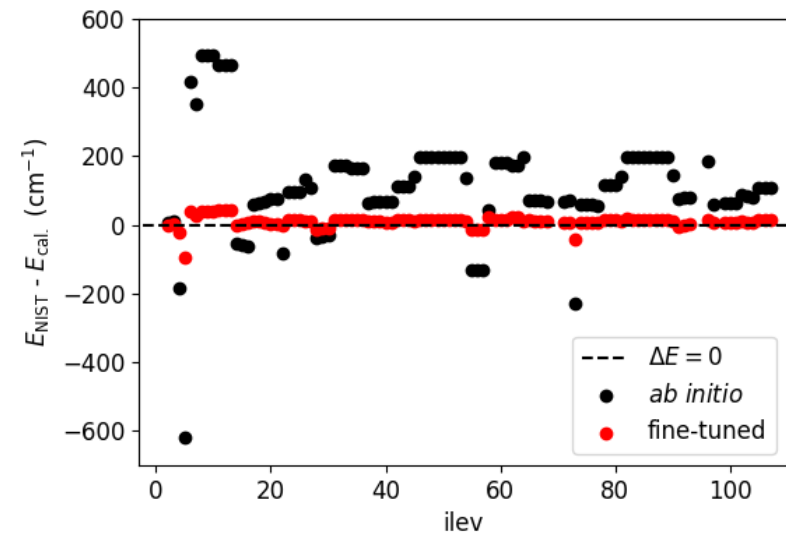
C abundance analysis
(Li et al. 2021)



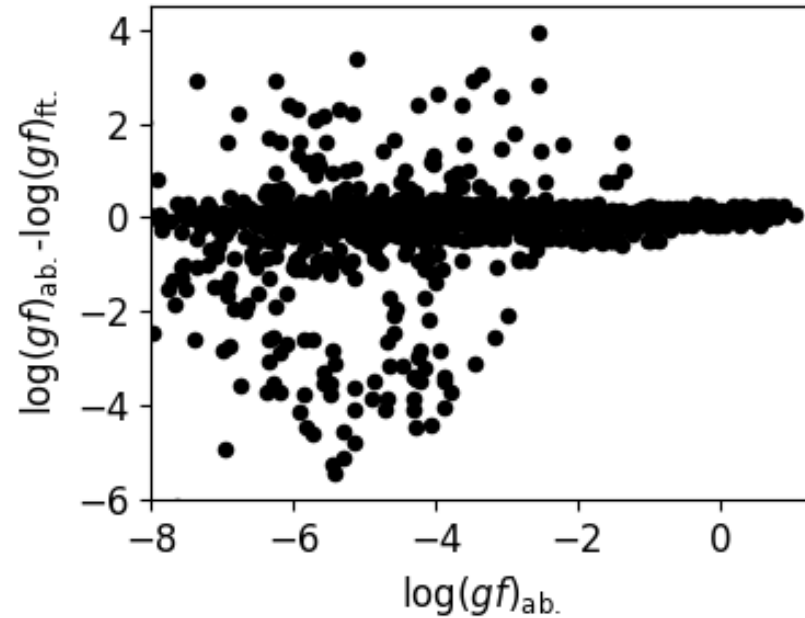
O abundance analysis
(Li et al. 2023)

GRASP calculations for radiative transitions

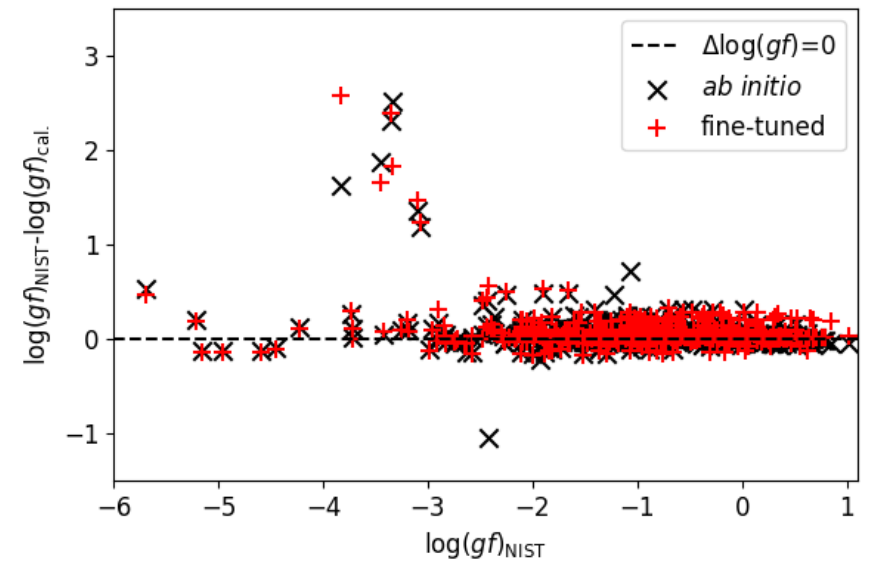
ab initio and fine-tuned energies and $\log(gf)$ for S I



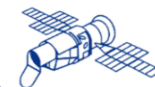
ab initio and fine-tuned energies compared with NIST-ASD



Comparison of *ab initio* and fine-tuned $\log(gf)$



ab initio and fine-tuned $\log(gf)$ compared with NIST-ASD



Theoretical calculations of collisional data

Collaborated with Connor Ballance and Tomas Brage

Atomic structure calculations: GRASP0 code

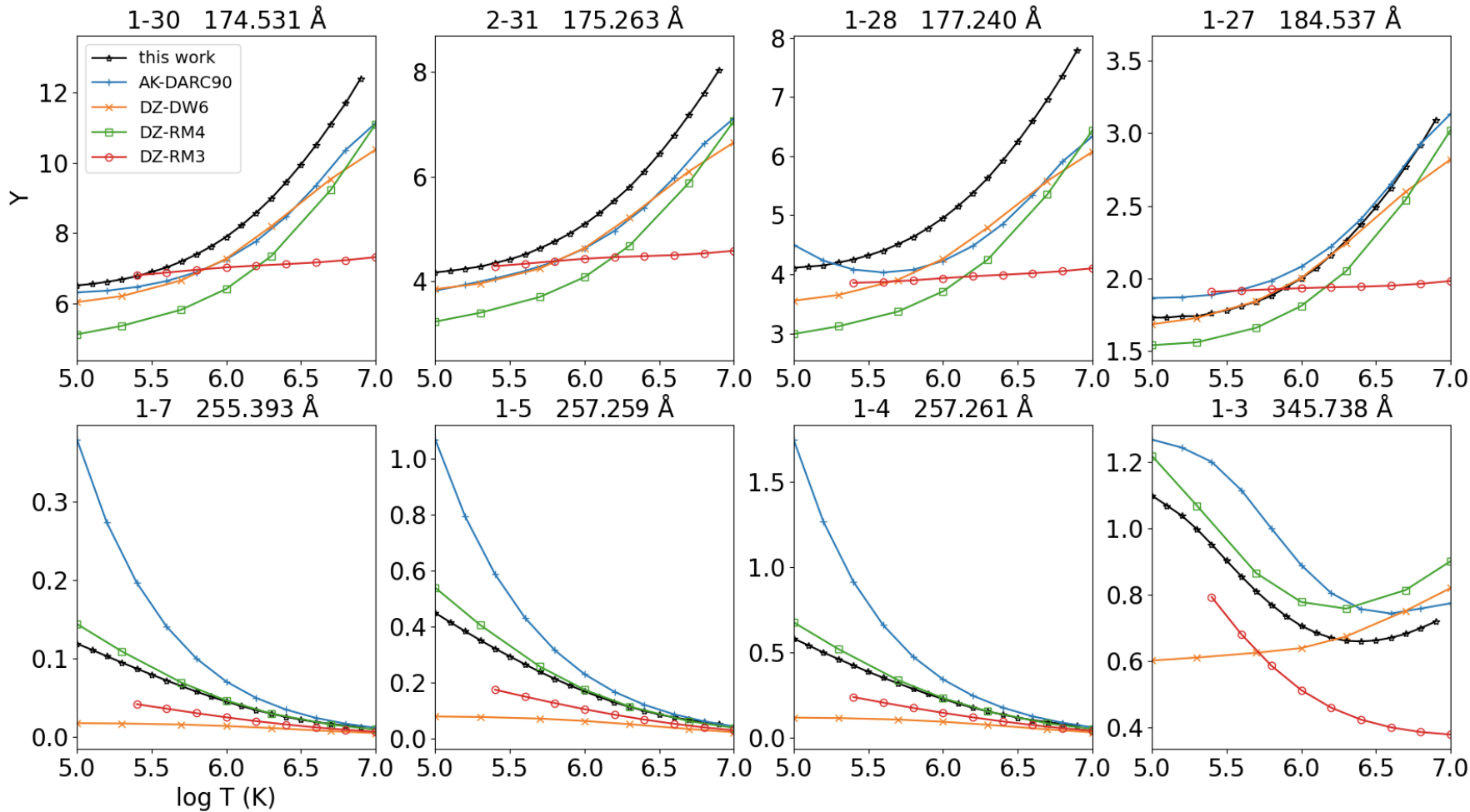
Scattering calculation: DARC codes based on the Dirac R-matrix method

i-j	λ (Å)	Lower level	Upper level	A (s ⁻¹)		Ratio
				CHIANTI V10.0 ^a	MCDHF ^b	
1-30	174.531	3s ² 3p ⁵ ² P _{3/2}	3s ² 3p ⁴ 3d ² D _{5/2}	1.860e+11	1.807e+11	0.97
2-31	175.263	3s ² 3p ⁵ ² P _{1/2}	3s ² 3p ⁴ 3d ² D _{3/2}	1.750e+11	1.697e+11	0.97
1-28	177.240	3s ² 3p ⁵ ² P _{3/2}	3s ² 3p ⁴ 3d ² P _{3/2}	1.540e+11	1.466e+11	0.95
1-27	184.537	3s ² 3p ⁵ ² P _{3/2}	3s ² 3p ⁴ 3d ² S _{1/2}	1.220e+11	1.249e+11	1.02
1-7	255.393	3s ² 3p ⁵ ² P _{3/2}	3s ² 3p ⁴ 3d ⁴ D _{1/2}	3.080e+06	3.453e+06	1.12
1-5	257.259	3s ² 3p ⁵ ² P _{3/2}	3s ² 3p ⁴ 3d ⁴ D _{5/2}	3.330e+06	6.077e+06	1.82
1-4	257.261	3s ² 3p ⁵ ² P _{3/2}	3s ² 3p ⁴ 3d ⁴ D _{7/2}	5.640e+01	5.748e+01	1.02
1-3	345.738	3s ² 3p ⁵ ² P _{3/2}	3s 3p ⁶ ² S _{1/2}	3.820e+09	2.996e+09	0.78

EUV lines in Fe X used for density, temperature and magnetic strength diagnostics



Theoretical calculations of collisional data



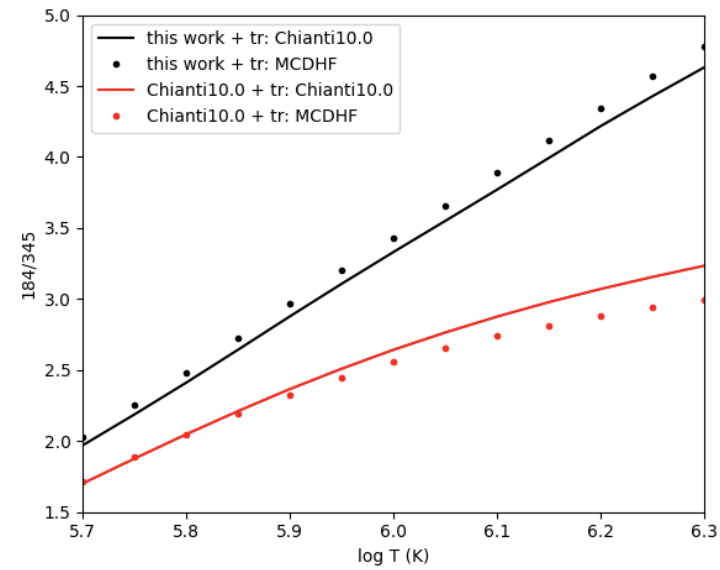
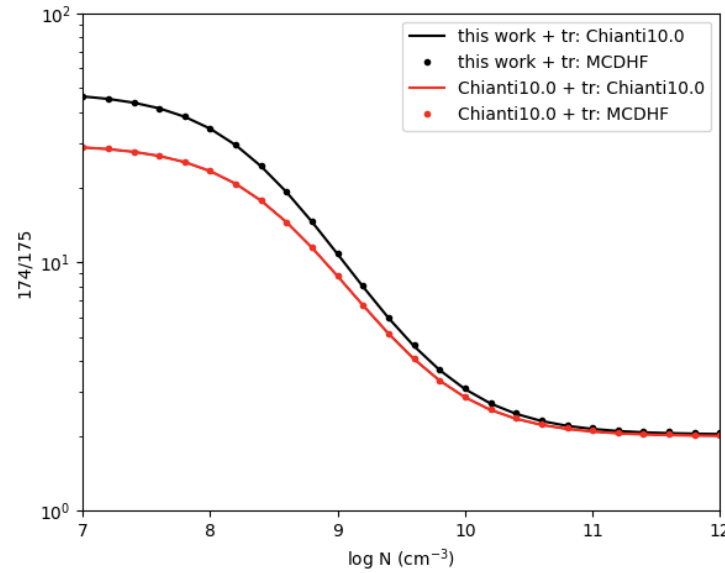
AK-DARC90: DARC R-matrix calculation from Aggarwal & Keenan (2005);
DZ-DW6: distorted wave calculation from Del Zanna et al. (2012);
DZ-RM4: R-matrix calculation from Del Zanna et al. (2012);
DZ-RM3: R-matrix calculation from Del Zanna et al. (2004);
This work: DARC calculation

Thermally-averaged effective collision strengths for Fe X lines, from different calculations.

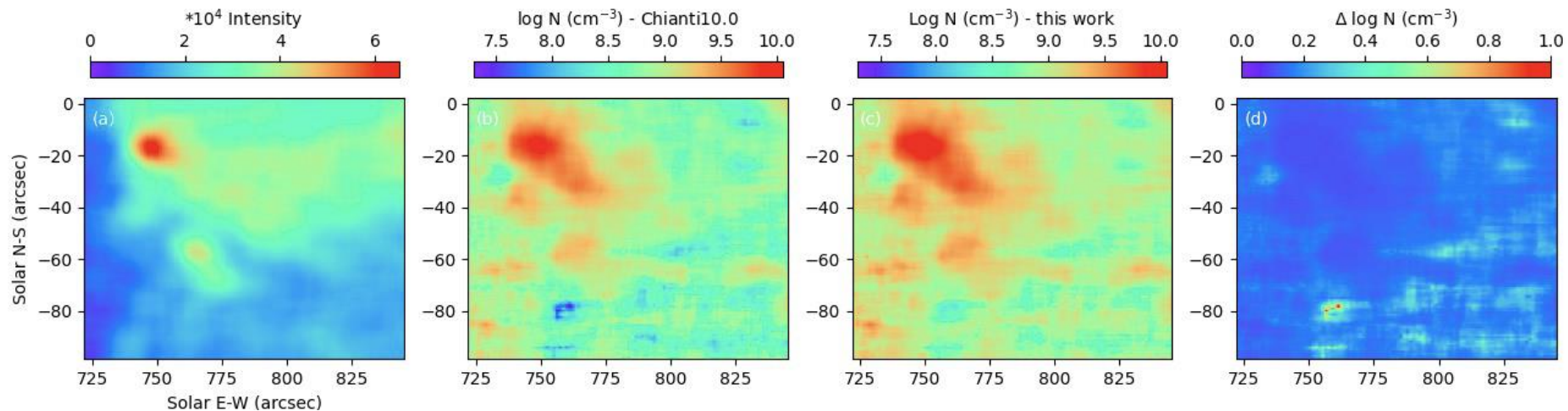


Theoretical calculations of collisional data

174/175 ratio as a function of electron density at temperature of 10^6 K \rightarrow



\leftarrow 184/345 as a function of temperature at electron density of 10^{10} cm^{-3}

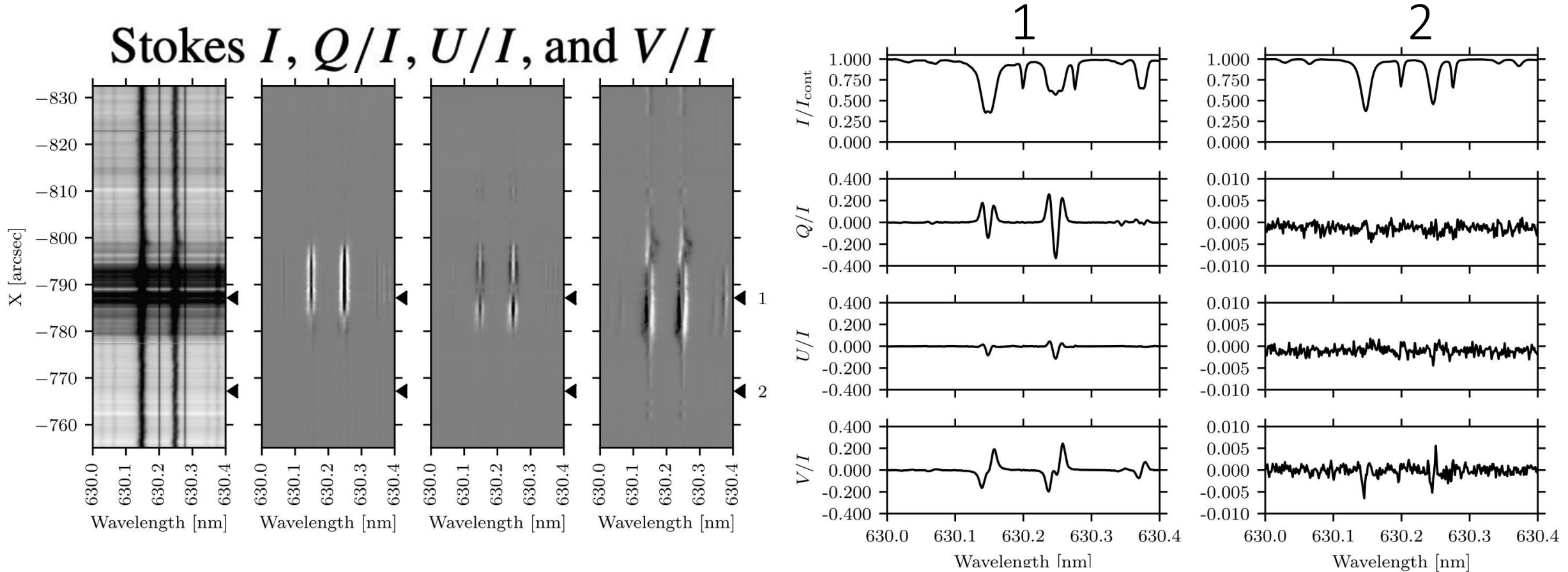


Density map obtained with different collisional data



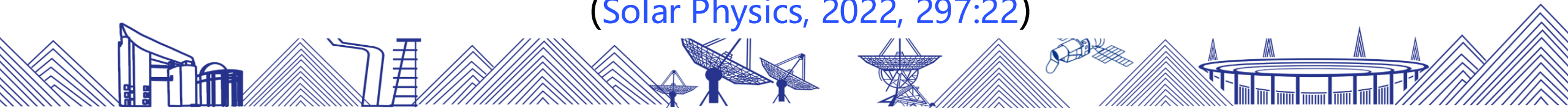


Spectropolarimetry: solar magnetic measurement



Fe I@630.2 nm from DKIST/ViSP

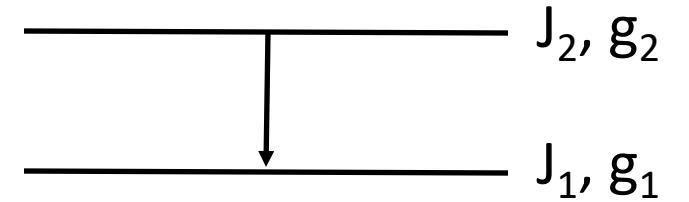
(Solar Physics, 2022, 297:22)



Landé factor

LS coupling, Zeeman induced polarization

“weak-field” approximation



$$\bar{g} = \frac{1}{2}(g_1 + g_2) + \frac{1}{4}(g_1 - g_2)d \text{ --- circular polarization}$$

$$\bar{G} = \bar{g}^2 - \delta \text{ --- linear polarization}$$

$$\delta = \frac{1}{80} \Delta^2 (16s - 7d^2 - 4) ,$$

$$d = J_1(J_1 + 1) - J_2(J_2 + 1) ,$$

$$s = J_1(J_1 + 1) + J_2(J_2 + 1) ,$$

$$\Delta = g_1 - g_2 .$$



Landé factor

LS coupling, Zeeman induced polarization

(1) Transitions with $\bar{g} \neq 0$ and $\bar{G} = 0$, which have zero *linear* polarization under the Zeeman effect;

$${}^4D_{1/2} - {}^{2S+1}L_{1/2}, {}^6G_{3/2} - {}^{2S+1}L_{1/2}, \text{ where } {}^{2S+1}L \neq {}^4D.$$

(2) Transitions with $\bar{g} = 0$ and $\bar{G} \neq 0$, which have zero *circular* polarization under the Zeeman effect;

$${}^6P_{3/2} - {}^4F_{5/2}, {}^5D_2 - {}^3G_3, {}^7D_1 - {}^5F_2, {}^8D_{5/2} - {}^6G_{7/2},$$

$${}^5F_2 - {}^5H_3, {}^7F_2 - {}^7H_3, {}^7F_3 - {}^5H_4, {}^8F_{3/2} - {}^6G_{5/2}.$$

(3) Transitions with $\bar{g} = \bar{G} = 0$, which have zero polarization under the Zeeman effect.

$${}^3P_0 - {}^5F_1, {}^4D_{1/2} - {}^4D_{1/2}, {}^4D_{1/2} - {}^6G_{3/2}, {}^5D_0 - {}^5F_1,$$

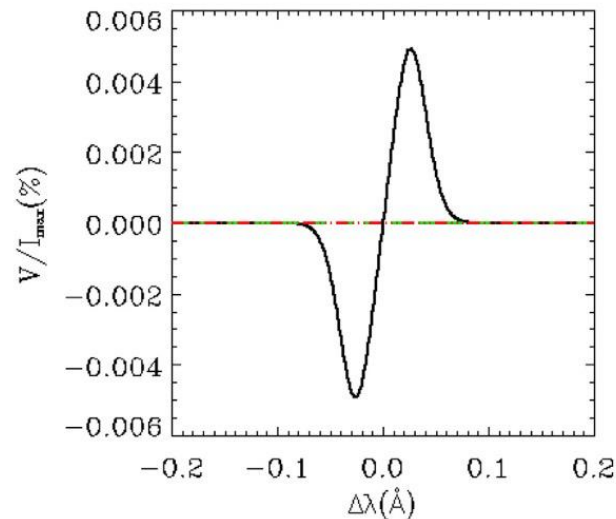
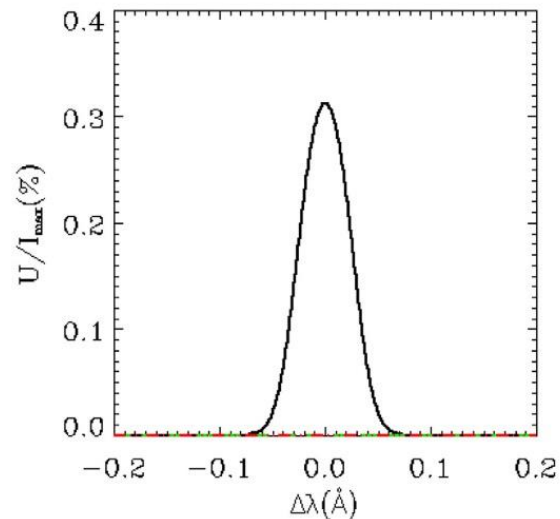
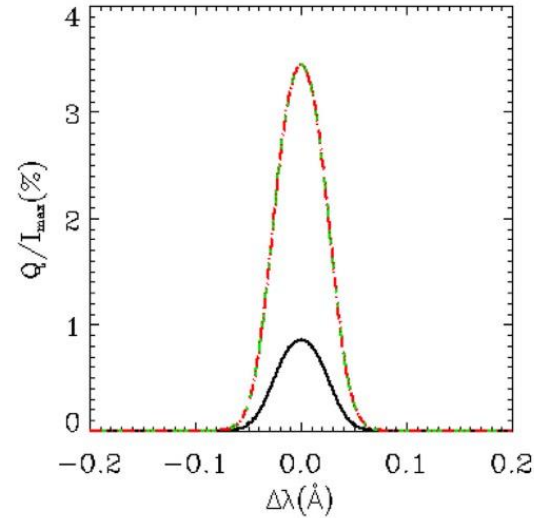
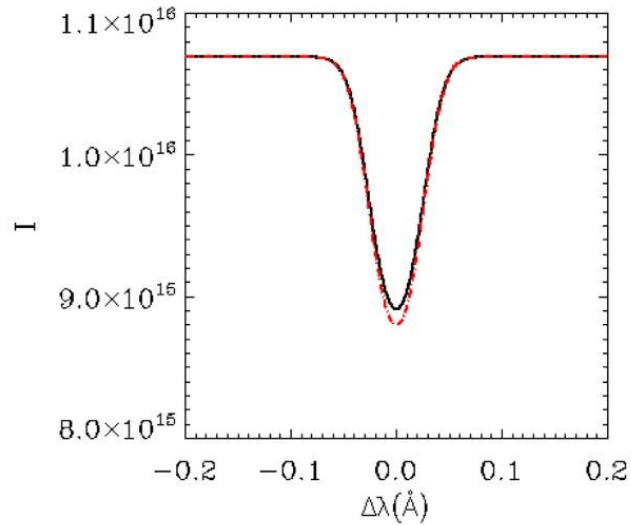
$${}^5F_1 - {}^5F_1, {}^5F_1 - {}^7F_0, {}^5F_1 - {}^7H_2, {}^6G_{3/2} - {}^6G_{3/2}, {}^7H_2 - {}^7H_2.$$

Transitions with large landé factor

$\bar{g}_{LS} \geq 3$					
${}^4P_{1/2} - {}^6D_{1/2}$	3.	${}^6D_{1/2} - {}^8F_{1/2}$	3.667	${}^8D_{5/2} - {}^6G_{3/2}$	3.6
${}^6P_{3/2} - {}^4D_{1/2}$	3.	${}^7D_1 - {}^7D_1$	3.	${}^8D_{7/2} - {}^6G_{5/2}$	3.
${}^6P_{3/2} - {}^6F_{1/2}$	3.167	${}^7D_1 - {}^7F_0$	3.	${}^7F_3 - {}^7H_2$	3.
${}^6P_{5/2} - {}^4F_{3/2}$	3.	${}^7D_2 - {}^5F_1$	3.	${}^7F_4 - {}^5H_3$	3.
${}^7P_2 - {}^5F_1$	3.5	${}^7D_2 - {}^7G_1$	3.25	${}^8F_{1/2} - {}^8F_{1/2}$	4.
${}^8P_{5/2} - {}^6F_{3/2}$	3.2	${}^7D_3 - {}^5G_2$	3.167	${}^8F_{5/2} - {}^6G_{3/2}$	3.
${}^5D_0 - {}^7D_1$	3.	${}^8D_{3/2} - {}^6F_{1/2}$	3.667	${}^8F_{5/2} - {}^8H_{3/2}$	3.3
${}^6D_{1/2} - {}^6D_{1/2}$	3.333	${}^8D_{3/2} - {}^8G_{1/2}$	3.833	${}^8F_{7/2} - {}^6H_{5/2}$	3.286



Landé factor



Stokes profiles of Fe I transition ${}^5F_1^0 - {}^5F_1$ at 7389.398 Å

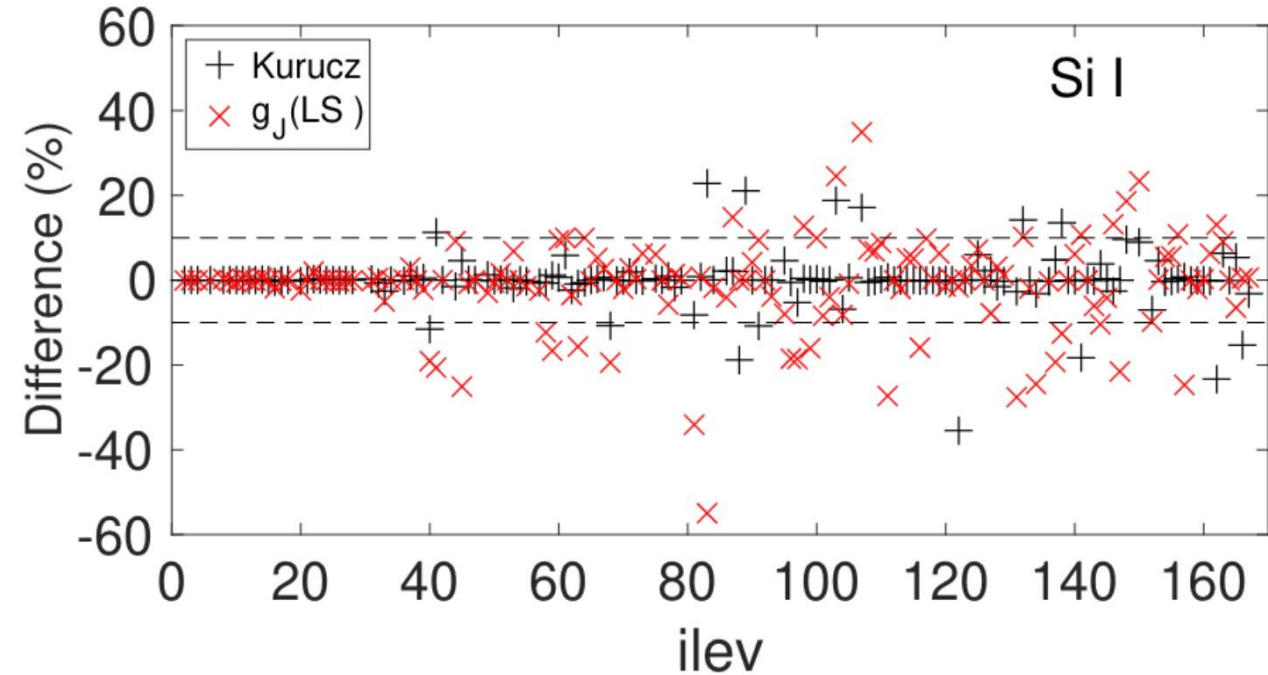
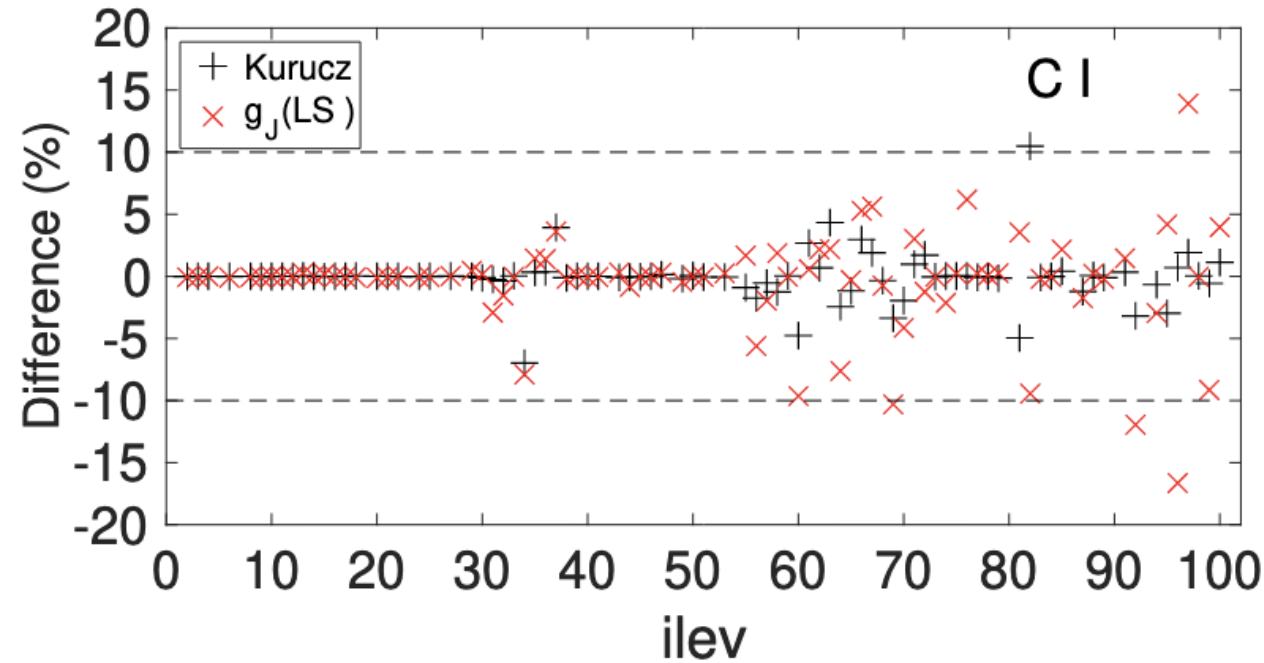
Red dashed curves: LS-coupling scheme $g_1 = g_2 = 0$, $B = 100$ G.

Green dashed curves: experimental $g_1 = -0.016$, $g_2 = 0.007$, $B = 0$ G

Black solid curves: experimental $g_1 = -0.016$, $g_2 = 0.007$, $B = 100$ G

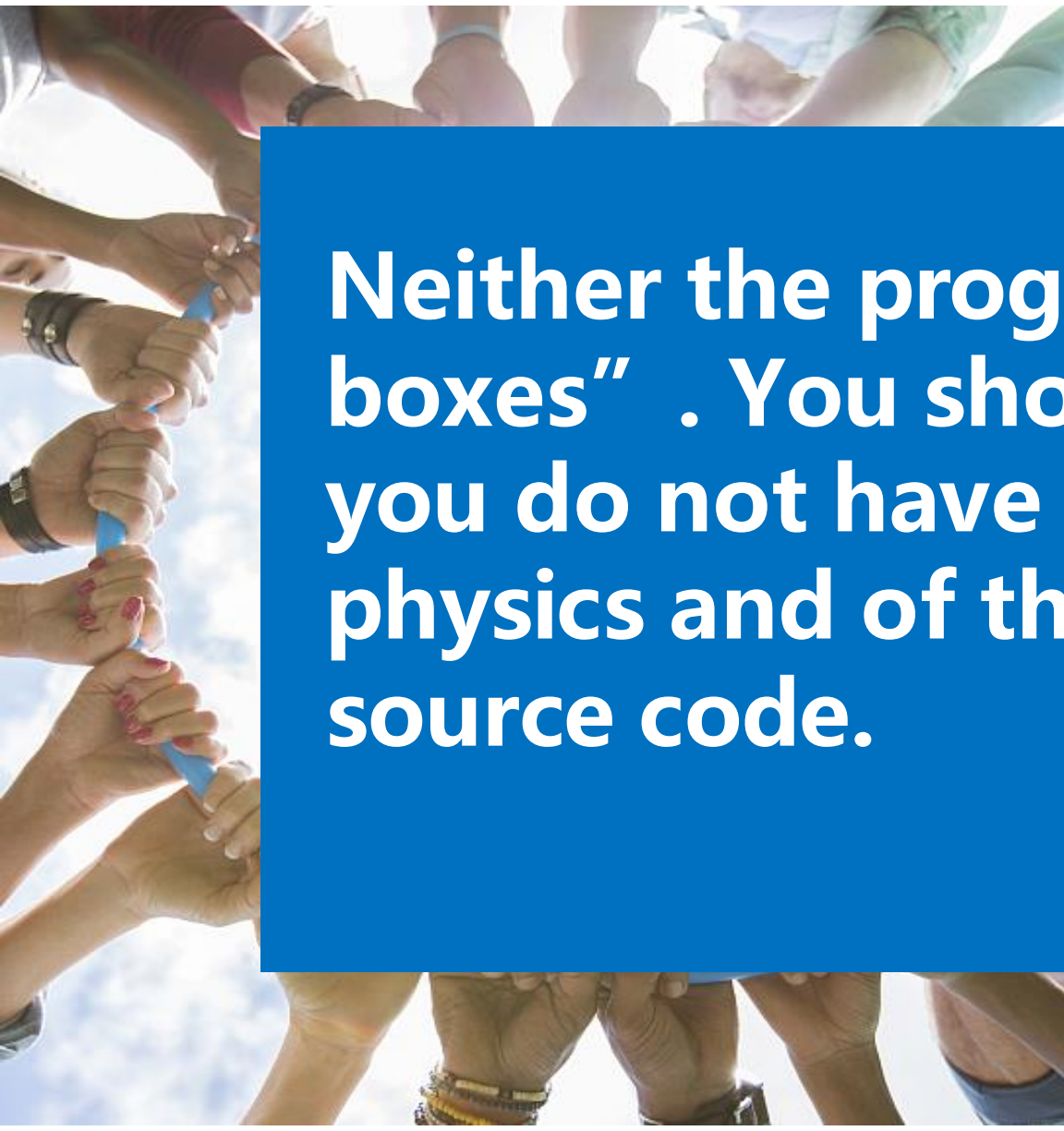


Landé factor calculations



MCDHF calculations of Landé factors compared with LS-coupling and Kurucz's database (<http://kurucz.harvard.edu/atoms.html>)



A photograph showing a group of people's hands reaching up from the bottom of the frame to hold a blue object, possibly a telescope component, against a bright, cloudy sky. The hands are of various skin tones and are wearing different accessories like watches and bracelets.

Neither the programs nor data are “black boxes” . You should not be using them if you do not have some understanding of the physics and of the programming in the source code.

--Robert L. Kurucz